Determining the first-order character of La(Fe,Mn,Si)$_{13}$

Milan Bratko,[1] Edmund Lovell,[1,*] A. David Caplin,[1] Vittorio Basso,[2] Alexander Barcza,[3] Matthias Katter,[3] and Lesley F. Cohen[1,†]

[1]*Blackett Laboratory, Imperial College London, Prince Consort Road, London SW7 2AZ, United Kingdom*

[2]*Istituto Nazionale di Ricerca Metrologica, Strada delle Cacce 91, 10135 Torino, Italy*

[3]*Vacuumschmelze GmbH & Co. KG, Hanau, Germany*

(Received 5 October 2016; revised manuscript received 16 January 2017; published 13 February 2017)

Definitive determination of first-order character of the magnetocaloric magnetic transition remains elusive. Here we use a microcalorimetry technique in two modes of operation to determine the contributions to entropy change from latent heat and heat capacity separately in an engineered set of La(Fe, Mn, Si)$_{13}$ samples. We compare the properties extracted by this method with those determined using magnetometry and propose a model-independent parameter that would allow the degree of first-order character to be defined across different families of materials. The microcalorimetry method is sufficiently sensitive to allow observation at temperatures just above the main magnetic transition of an additional peak feature in the low field heat capacity associated with the presence of Mn in these samples. The feature is of magnetic origin but is insensitive to magnetic field, explicable in terms of inhomogeneous occupancy of Mn within the lattice resulting in antiferromagnetic ordered Mn clusters.

DOI: 10.1103/PhysRevB.95.064411

I. INTRODUCTION

La(Fe,Si)$_{13}$ based compounds are promising candidates for solid state magnetic cooling, exhibiting a large magnetocaloric effect (MCE) associated with a metamagnetic first-order phase transition (FOPT) above the Curie temperature T_C, and are attractive due to their being made up mainly of highly abundant materials as well as potentially offering modest magnetic and thermal hysteresis. The T_C is tunable by substitution onto the Fe site. T_C increases with increasing Si content, for example [1,2], and the sharp features observed in magnetization for low Si concentrations broaden as the material moves from a first order to a continuous phase transition. Strong first-order materials show thermal and magnetic hysteresis, which limits the available entropy and adiabatic temperature changes available in the refrigeration cycle, and also introduces loss [3–5]. T_C can also be shifted to near room temperature by hydrogen absorption while sustaining the large MCE [6,7]. Partial replacement of Fe by other transition metal elements such as Mn, Co, Cr, and Ni, and interstitial atoms such as B, C, N, and H have been explored both experimentally and theoretically [8]. Most commonly, a combination of Mn substitution, Si composition, and absorption of interstitial hydrogen (referred to as hydrogenation) is used to optimize the magnetocaloric properties, bringing the transition as close to first order as possible while engineering a range of T_C so that a cascaded set of solid state refrigerants can be employed, for refrigeration applications with a useful range of working temperatures [9–12]. Previously, the LaFe$_x$Mn$_y$Si$_{13-x-y}$ system was studied as a function of Mn content. It was found that T_C decreased monotonically with increasing Mn concentration from 188 to 127 K, and the saturation magnetization m_{sat} decreases from 23.9 to 22.2 μ_B/f.u., respectively, as y increases from 0 to 0.35 [9]. The decline of m_{sat} was found to be faster than simple magnetic dilution. This may have two causes. One is that the magnetic moment per Fe atom is reduced due to the change of Fe chemical environment caused by the Mn substitution. The other is that the Mn atoms carry magnetic moments that couple antiparallel to the Fe moments. The latter has been recently confirmed theoretically [8], but is at variance with an experimental study using Mössbauer spectroscopy [13].

La(Fe,Si)$_{13}$ is an itinerant ferromagnet, showing a critical point T_{crit} in its H-T phase diagram. At temperatures and fields below T_{crit}, the transition between paramagnet and ferromagnet is first order in character, showing thermal and magnetic hysteresis. Above T_{crit}, the transition shows the signatures of a continuous phase transition, no intrinsic hysteresis, and significantly broadened features. There are a number of models based on the Landau expansion of the free energy used to parametrize the order of the transition: the Banerjee criteria [14], the Arrot plot [15], the Bean Rodbell model [16] and its extensions [17], and for itinerant systems, spin fluctuation theory [18,19]. However, most of these models require a number of parameters to be defined including those related to real materials, such as an inhomogeneous spread of T_C and clustering [20]. It is difficult to compare first-order character between materials when different models apply to different types of magnetic systems (local and itinerant magnetism). Although hysteresis is considered to be a signature of first-order character, we have previously shown that there can be also extrinsic contributions to hysteresis [21,22], and that the relationship between latent heat and hysteresis is different for different material families [23]. Consequently a direct measure of the degree of first-order character is lacking.

Recently the tuning of T_{crit} was explored in a series of La(Fe, Mn, Si)$_{13}$-H$_{1.65}$ from the characteristic changes in heat capacity [24]. In this paper we consider the matching family of La(Fe, Mn, Si)$_{13}$ materials (that is, without the hydrogenation). We consider the order of the transition by extracting the latent heat explicitly and show how it is suppressed in applied magnetic field as the critical point is approached. We show the influence of interstitial hydrogen on

*Corresponding author: e.lovell12@imperial.ac.uk

†Corresponding author: l.cohen@imperial.ac.uk

TABLE I. Summary of the T_C and compositions of the series of $LaFe_xMn_ySi_z$ compounds studied. All samples are the dehydrogenated compositions, except sample B (with H) where $H = 1.65$.

Sample	A	B	C	D	E	F	G	B (with H)
T_C (K)	110	131	142	150	158	168	173	283
X (Fe)	11.22	11.33	11.41	11.49	11.58	11.66	11.74	11.33
Y (Mn)	0.46	0.37	0.30	0.23	0.18	0.12	0.06	0.37
Z (Si)	1.32	1.30	1.29	1.27	1.25	1.23	1.20	1.30

this behavior in one sample that has been hydrogenated. For a representative set of samples we compare the latent heat in field with the information that can be extracted from magnetization using the Clausius-Clapeyron equation and Maxwell relations [25], and use this to define a model independent parameter of first-order character Ω. The ac calorimetry measurements reveal an additional feature which we interpret as being due to antiferromagnetic regions in the sample of the order of 20% of the total volume due to Mn clusters.

II. EXPERIMENTAL METHOD

A. Samples

$La(Fe, Mn, Si)_{13}$ alloys with variable Mn content were prepared by powder metallurgy techniques and, in the case of one of the compositions, hydrogenated as described in Ref. [10]. Master alloys were prepared by vacuum induction melting followed by mechanical milling steps to produce fine powders. The composition of each alloy was adjusted by blending master alloys with elemental powders. Compaction of the powder blends was performed by cold isostatic pressing. The green bodies were vacuum sintered at around 1100 °C followed by an annealing treatment at 1050 °C [26]. Hydrogenation was performed on a granulate material with a particle size less than 1 mm by heating to 773 K in argon. At 773 K argon was replaced with hydrogen followed by a slow cool to room temperature. The compositions are summarized in Table I.

B. Magnetometry

All magnetization measurements were performed using a Quantum Design PPMS VSM option with an external magnetic field up to 9 T. The magnetization as a function of temperature for samples A–G are shown elsewhere [27]; here for brevity we show a representative set of magnetization versus field curves as a function of temperature for sample E in Fig. 1(a).

The isothermal entropy change $\Delta S_{\mathrm{Maxwell}}$ was obtained from isothermal magnetization measurements using the Maxwell relation

$$\left(\frac{\partial S}{\partial B}\right)_T = \left(\frac{\partial M}{\partial T}\right)_B, \tag{1}$$

where M is the magnetization and B is the magnetic flux density, which we assume to be equal to $\mu_0 H$. In the vicinity of a hysteretic first-order phase transition (FOPT), a measurement protocol consistent with Ref. [28] has been adopted in order to avoid nonphysical overestimates of the isothermal entropy change [29].

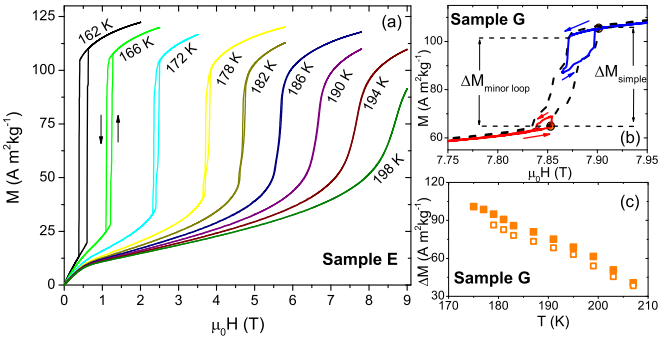

FIG. 1. (a) Magnetization as a function of applied magnetic field for composition E for various T above T_C. Example arrows at one T show the direction of movement around the hysteresis loop. (b) The field-driven transition of sample G at 207 K (dashed) indicating the definition of ΔM, with an example of the minor loop method approaching from the low field state (red) and the high field state (blue) and the commencement of the irreversibility region. This allows accurate determination of the hysteretic region and therefore ΔM corresponding to the FOPT. (c) Extracted ΔM values from the simple (closed) and minor loop (open) methods.

In order to estimate the latent heat contribution to the total entropy change from the magnetization data we have used the Clausius-Clapeyron equation:

$$\Delta S_{\mathrm{CC}} = -\Delta M \mu_0 \frac{dH_C}{dT}, \tag{2}$$

where ΔM is the change in magnetization at the FOPT, i.e., the part of the M-H curve representing the field driven metamagnetic transition where there is irreversibility (note that there are also reversible changes in M immediately above and below the FOPT) and first-order discontinuity in M. Note also that the FOPT has a finite width in field, because demagnetizing effects introduce field inhomogeneity; we take the critical field H_C as the midpoint of the irreversible section of the transition at temperatures above T_C (the zero field critical temperature), and $\mu_0 dH_C/dT$ as the slope of the phase line of the FOPT. Calculating accurate ΔM values can be difficult and inconsistent, particularly for weakly first-order transitions where the region of first-order transition is not explicit, for example when there are extrinsic contributions to hysteresis [22] and extrinsic broadening of the transition such as that caused by field inhomogeneity. To account for this, in addition to a simple calculation of ΔM measured as the difference in M at the beginning and end of the hysteretic region (taken on field application), we also perform minor M-H hysteresis loops to establish the precise value of H and corresponding M at which irreversibility (hysteresis) sets in. This is achieved as follows: both the transitions on field application and field removal are separately approached, before returning the field to its original value. This is performed for a number of set field values close to the transition until irreversibility between increasing and decreasing applied field occurs. Figures 1(b) and 1(c) demonstrate these methods and give an example of the estimated ΔM values taken from each, respectively, for sample G.

C. Microcalorimetry

Microcalorimetry measurements were performed using a commercial Xensor SiN membrane chip (TCG-3880) adapted to operate either as an ac calorimeter [30] or as a quasiadiabatic temperature probe [31], in a cryostat with temperature range 5–293 K and an external magnetic field up to 8 T. The sample is a fragment of the bulk, typically ∼100 μm with mass of the order of few μg. For an accurate determination of mass, the fragments were measured in the magnetometer and the saturation magnetization of the ferromagnetic state was compared with bulk samples of known mass. The low temperature specific heat data for the same compositions summarized in Table I have been discussed elsewhere [27].

In the ac measurement a modulated power is applied to the sample and the heat capacity is determined from the phase and amplitude of the resulting small temperature oscillations, which are measured using a lock-in amplifier. Thus the technique measures only reversible changes in heat capacity and the latent heat is ignored because of the hysteresis associated with it. The ac heat capacity measurement is absolute: however, the sensitivity of the thermopile used to measure the temperature oscillations has to be calibrated. For this purpose the temperature dependence of the heater resistance is used as a reference measure of temperature. Nevertheless, due to the finite thermal resistance between the heater and the sample, the heater is always hotter than the sample and a fixed correction factor has to be applied to the thermopile sensitivity. The correction factor can be determined by comparing field induced entropy changes estimated from the ac heat capacity data and magnetization measurements. This was performed well away from the first-order phase transition, where both techniques should work reliably and produce comparable estimates.

Figure 2(a) shows the heat capacity measured as a function of temperature. The heat capacity can be used to calculate the entropy change ΔS. For a field variation from 0 T to $\mu_0 H$:

$$\Delta S(T) = \Delta S(T_{\rm ref}) + \int_{T_{\rm ref}}^{T} \frac{C_{p,\mu_0 H}(T) - C_{p,0}(T)}{T} dT, \quad (3)$$

where the reference entropy change at $T_{\rm ref}$ can be obtained from magnetization measurements. The zero field and in-field heat capacity values used are both from either cooling or heating curves.

As explained in Ref. [32], because the ac calorimeter measurement excludes the latent heat, comparison of the entropy change determined by the ac calorimeter method with the total magnetic entropy change estimated from magnetization measurements $\Delta S_{\rm Maxwell}$ can be used to estimate the latent heat indirectly.

In order to reflect the total entropy change above T_C, Eq. (3) can be modified to

$$\Delta S(T_C < T < T_H) = \Delta S(T_{\rm ref}) + \int_{T_{\rm ref}}^{T} \frac{C_{p,\mu_0 H}(T) - C_{p,0}(T)}{T} dT + \Delta S_{\rm LH}(T_C) \quad (4)$$

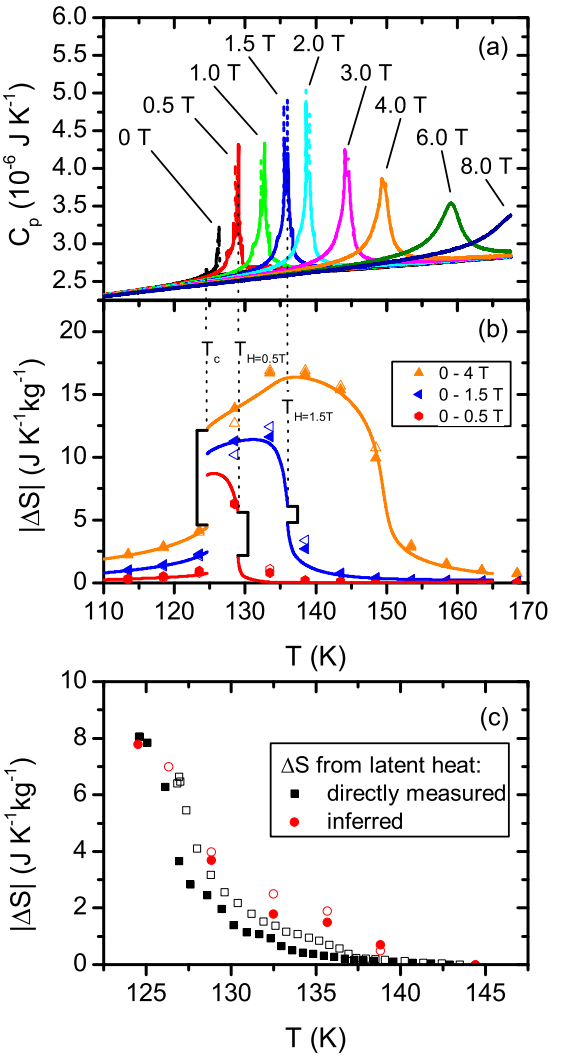

FIG. 2. (a) The ac heat capacity of sample B (without hydrogen) as measured in the microcalorimeter. (b) These entropy changes calculated from the ac heat capacity on cooling (lines) exclude the latent heat contribution and therefore require offsetting above T_C and T_H (the latter varies based on the upper field limit) in order to fit the total magnetic entropy change as estimated from the magnetization measurements (symbols) using the Maxwell relation. The manually fitted offsets (indicated by the brackets) offer an indirect measure of the entropy change associated with the latent heat. (c) ΔS from directly measured latent heat compared with that inferred from ac heat capacity data. For (b) and (c), solid lines and symbols correspond to cooling or field application and dashed/open lines and symbols correspond to heating or field removal.

and

$$\Delta S(T > T_H) = \Delta S(T_{\rm ref}) + \int_{T_{\rm ref}}^{T} \frac{C_{p,\mu_0 H}(T) - C_{p,0}(T)}{T} dT + \Delta S_{\rm LH}(T_C) - \Delta S_{\rm LH}(T_H), \quad (5)$$

where $\Delta S_{\rm LH}$ is the entropy change associated with the latent heat released at T_C and T_H for temperature sweeps in 0 T and $\mu_0 H$, respectively. $\Delta S_{\rm LH}(T_C)$ and $\Delta S_{\rm LH}(T_H)$ can be used

as fitting parameters. An example of this fitting procedure is shown in Fig. 2(b).

The microcalorimeter enables also a direct measurement of the latent heat in the quasiadiabatic temperature probe setup which relies on the instantaneous release of latent heat as the sample is driven monotonically through the first-order phase transition either by applying magnetic field or changing the temperature. The release of latent heat results in a sharp change of temperature of the sample (and addenda). This is recorded as a sharp spike in thermopile voltage with an exponential decay as the latent heat diffuses to bath. The temperature spike can be described by

$$\Delta T = \frac{Q_{\mathrm{LH}}}{C} e^{-\frac{G}{C}t}, \tag{6}$$

where Q_{LH} is the latent heat released, C is the heat capacity of the sample and the addenda, and G is the thermal conductance between the sample and the bath. In order to maximize the reproducibility of the measured peak height for a given amount of latent heat, the time constant is lengthened by evacuating the sample space to below 4×10^{-2} mbar and thus reducing the thermal link to bath.

In the original measurement setup [32], the peak height was used as the measure of latent heat, calibrated by a reference heat pulse of known energy from a local heater. This approach assumes that C does not vary significantly between the measurement and the calibration. Nevertheless, in Fig. 2(a) it can be seen that in the samples studied here the background heat capacity may vary by as much as 100% at the first-order phase transition when the latent heat is released. For this reason we have considered the area of the peak as a more reliable measure of latent heat as opposed to the peak height—the integral of Eq. (6) yields $Q_{\mathrm{LH}}G$, where G can be expected not to vary with the applied field and vary only slightly over a small temperature range. Furthermore, the integration approach simplifies the data analysis in samples where a cascade of overlapping peaks is observed, as the successive peaks superimpose linearly and the whole cascade can be simply integrated.

This approach has been validated by performing a calibration in zero field away from a phase transition and at the same temperature in-field, in the vicinity of the heat capacity peak. While the height of the calibration peak varied significantly, the area of the calibration peak remained unaffected by the change in background heat capacity.

Figure 2(c) shows the thus evaluated directly measured latent heat compared with the latent heat inferred indirectly from the comparison of ac heat capacity data with Maxwell-relation derived results from magnetization. The two are in good agreement, thus validating the measurement method as well as our approach to separate the first-order contribution to the total entropy change.

III. RESULTS AND DISCUSSION

In Fig. 3 we show the changes of heat capacity and latent heat in sample E. When the system approaches the critical point, the latent heat drops to zero and, characteristically, we see an increasing peak in the ac heat capacity [33,34]. Thus, while the total entropy change maintains a plateaulike

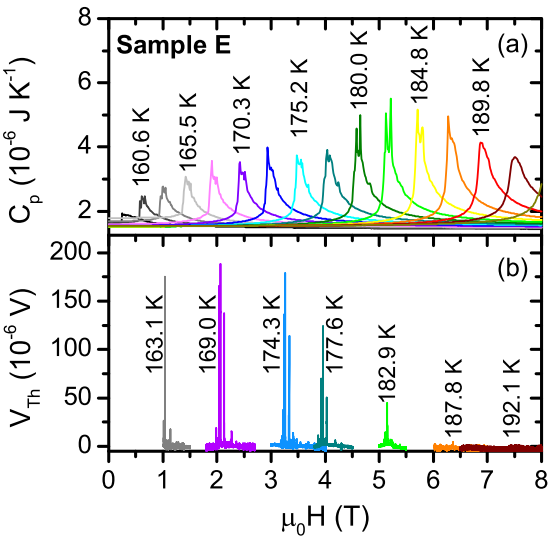

FIG. 3. ac heat capacity (a) increases with field/temperature while the latent heat signal (b) diminishes as the metamagnetic phase transition approaches criticality and becomes continuous, as shown for sample E.

shape typical for a first-order phase transition, the first-order contribution gradually decreases. After the transition becomes fully continuous, the peak in heat capacity broadens and subsides.

In order to evaluate the critical point a measure often used is the point of vanishing thermal/field hysteresis [24]. Figure 4 shows the T_C and the T_{crit} across the series using this method. The T_{crit} has been identified as the point of vanishing hysteresis in the specific heat measurement for the hydrogenated samples (as reported in Ref. [24]), and in the magnetization measurements for the samples without hydrogen. It can be observed in Fig. 4(a) that T_C changes systematically with introduction of Mn and that the same is true of the hydrogenated samples with their much higher T_C. The variation of T_C with Mn is not greatly affected by hydrogenation, but both Mn and hydrogen significantly tune the critical point. Indeed in this sample series, the temperature separation between T_C and T_{crit} could be used as a measure of first-order strength of the transition. It can be seen that both Mn and H systematically weaken the first-order character (i.e., T_{crit} approaches T_C).

Figure 4(b) shows the phase lines for the dehydrogenated series and Fig. 4(c) shows the derivatives $\mu_0 dH_C/dT$. It has been discussed elsewhere [35–37] that there is an optimum value of $\mu_0 dH_C/dT$ to achieve maximum entropy change, where it is assumed that $\mu_0 dH_C/dT$ is field invariant, which is clearly not the case here. We return to this point later. Using the direct latent heat measurement we can obtain significantly more detail on how the critical point is approached across the series and under the influence of hydrogen. We focus on samples B, E, and G in the state without hydrogen and consider the effect of hydrogenation on sample B.

Figures 5(a)–5(d) compare the directly measured latent heat contribution to the entropy change and the entropy change $\Delta S_{\mathrm{Maxwell}}$ estimated from bulk magnetization measurement for 0 to 1.5 T and 0 to 8 T [using the Maxwell relations, Eq. (1)].

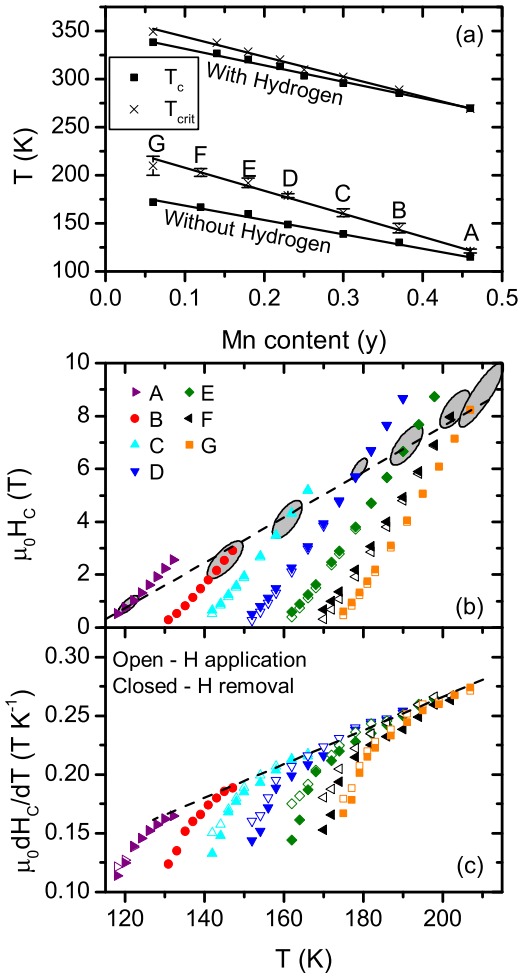

FIG. 4. (a) T_C and T_{crit} as a function of Mn doping in the samples with and without hydrogen. The data set with hydrogen was taken from Ref. [24]. Phase lines (b) and their slope (c) derived from the bulk magnetization data for the samples without hydrogen. The critical point was determined from the point where the phase lines on field application and removal converge. The shaded areas in (b) indicate the uncertainty in the critical point temperature and solid and open symbols in (b) and (c) correspond to field application and field removal, respectively.

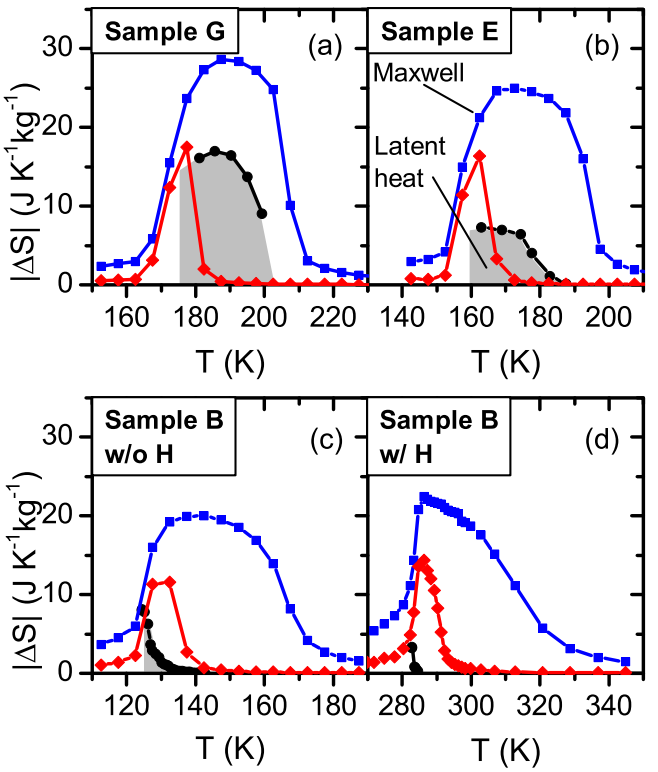

FIG. 5. Directly measured latent heat contribution to entropy change (black circles) at the FOPT compared with $\Delta S_{Maxwell}$ calculated from magnetization measurements for a magnetic field variation of 0 to 1.5 T (red diamonds) and 0 to 8 T (blue squares). All data correspond to magnetic field application/cooling.

For increasing field ranges, the ΔS value at the plateau increases. A small contribution is due to the fact that the α-Fe produces a high field slope to the magnetization, but the main reason is that there is also a contribution from the ferromagnetic phase close to the transition which increases for larger field ranges and as T increases the contribution of the purely paramagnetic phase also increases [38]. The latent heat contribution to the entropy change decreases with increasing Mn content as the T_C and T_{crit} are brought closer.

In the most strongly first-order sample G, the latent heat contribution to entropy change shows an initial small increase at T_C, followed by a broad plateau and then a sharp decline. In the sample with higher Mn content E, the plateau is lower in absolute value and shows a similar sharp decline. In the highest Mn content sample B only the sharp decline remains.

Figure 6 shows the direct influence of hydrogenation on sample B. Interestingly the magnitude of the latent heat at

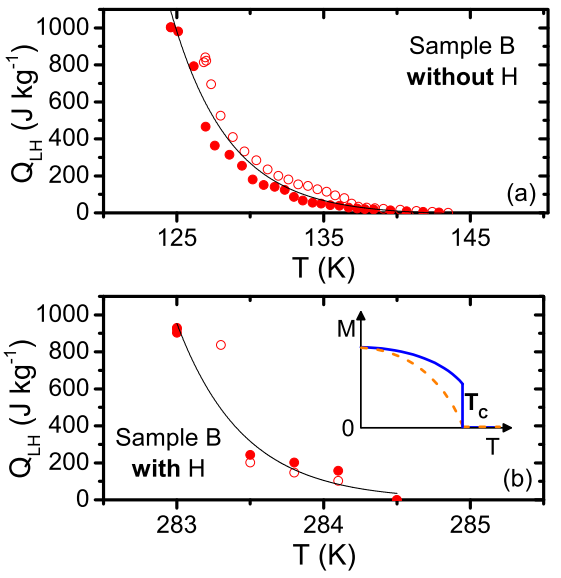

FIG. 6. The latent heat measured in sample B (a) without hydrogen and (b) with hydrogen. Solid symbols correspond to cooling/field application, open symbols correspond to heating/field removal. The lines correspond to an exponential decay fit. The decay is approximately 10 times faster in the hydrogenated state. Inset: Schematic of the $M(T)$ behavior of a first-order (solid) and continuous (dashed) ferromagnet to paramagnet phase transition.

T_C is comparable in the two sample states. The sharp decay is exponential in both cases, showing that there is a region approaching T_{crit} where the evolution is a thermally driven process and 10 times faster in the hydrogenated state at higher T (see Fig. 6).

Much of the literature on magnetocalorics refers to materials that show strongly or weakly first-order character. However, this is an ill-defined quantity with different meaning depending on the model used to analyze the material system. We introduce a generic model independent parameter which could in principle be used to compare the first-order character of the transition between material families. Although, as we show in Fig. 4(a), in $La(Fe,Si)_{13}$ there is a well-defined T_{crit} and a parameter based on $(T_C - T_{\text{crit}})$ could be used as a measure of the strength of first-order properties, not all magnetocaloric families show a critical point in their phase diagram (indeed it appears only in those materials with itinerant character that have a critical point attainable with magnetic fields available in standard laboratory environments). Consequently as $(T_C - T_{\text{crit}})$ is not sufficiently generic, we suggest a parameter that is based on the direct measure of the latent heat contribution to the entropy change as a fraction of $\Delta S_{\text{Maxwell}}$. We suggest a simple normalization procedure so that for a purely continuous transition (no latent heat), the parameter is zero, and if all the entropy change is captured by the latent heat, the parameter is 1. From Fig. 5 we learn that in the metamagnetic transition, the strength of the first-order character changes with increasing magnetic field (true particularly for materials exhibiting a T_{crit}). Studying the trends in Figs. 5 and 6 suggest that at the zero field T_C, for $La(Fe,Si)_{13}$, the latent heat carries almost all the entropy change, but the strength of the magnetoelastic coupling weakens at higher temperature and field. We write the parameter as $\Omega(B)$:

$$\Omega(B) = \frac{\int_{T_1}^{T_2} (\Delta S_{\text{CC}})_B dT}{\int_{T_1}^{T_2} (\Delta S_{\text{Maxwell}})_B dT}, \tag{7}$$

where T_1 (low) and T_2 (high) are temperatures well into the ferromagnetic and paramagnetic states of the material, respectively, and B is the maximum of the field range. ΔS_{CC} corresponds to the first-order contribution to the entropy change only and will be zero for continuous phase transitions. The entropy change determined from the Maxwell relation $\Delta S_{\text{Maxwell}}$ includes both the first-order and continuous contributions to the entropy change in a magnetic field B. If we assume that the transition has magnetostructural or magnetoelastic coupling and that the entropy change determined from the Maxwell relation reflects the total entropy change over the transition, this same total entropy change could also be measured by differential scanning calorimetry, in which case $\Delta S_{\text{Maxwell}}$ should be replaced by ΔS_{total} in Eq. (7).

In order to explore the use of the Ω parameter we use the latent heat determined estimation of the Clausius-Clapeyron component ΔS_{CC} and the magnetization determined value $\Delta S_{\text{Maxwell}}$ to obtain values for $\Omega(1.5\,\text{T}) = 0.73, 0.37$, and 0.16 for samples G, E, and B (without hydrogen), respectively. Further to this we investigate whether the same information that we have gathered from the latent heat can be extracted directly from magnetization-field curves using the Clausius-Clapeyron (CC) Eq. (2). The inset to Fig. 6 shows a schematic

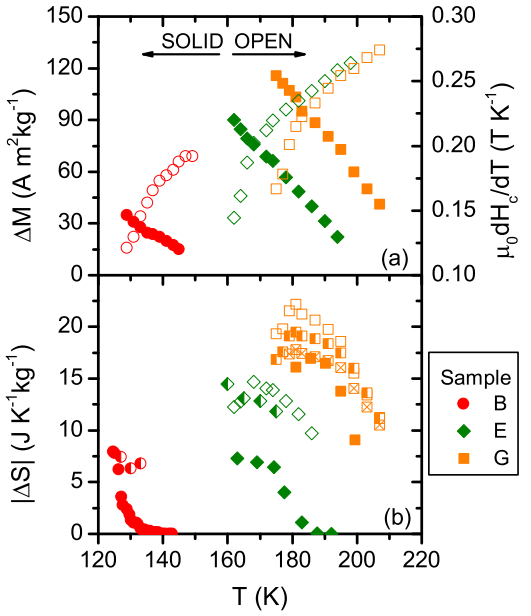

FIG. 7. (a) ΔM (taken from the onset of hysteresis) and $\mu_0 dH_C/dT$ variation as a function of temperature taken from bulk samples (without hydrogen). (b) ΔS from directly measured latent heat (solid symbols) compared with that from the Clausius-Clapeyron equation [ΔS_{CC}, Eq. (2)] using ΔM taken from the onset of hysteresis (open and half-filled symbols for bulk and fragment data, respectively) and from minor hysteresis loops on a fragment of sample G (crossed squares). All data correspond to magnetic field application/cooling.

of a transition with first-order and continuous character. Equations (1) and (2) do not yield the same result for these transitions. In the case of a continuous transition the entropy change determined by Eq. (2) would be zero, as there is no sharp jump at T_C, whereas the value would be finite using Eq. (1). For a purely first-order transition, the two equations should yield identical results. Essentially, the Ω parameter is a numerical measure of this difference.

It is interesting to explore the estimation of ΔS_{CC} using magnetization rather than latent heat, as has been proposed previously [38]. Equation (2) requires the product of the derivative of the phase line and the sharp change of ΔM at the transition. Figure 7(a) shows the phase line derivative and the estimated ΔM. As discussed above, it is usually assumed that the slope of the phase line is constant or varies only very little. An added complication is that this is not the case in the samples studied here as shown in Fig. 4(c) and repeated here for samples B, E, and G. The slope of the phase line varies significantly in a trend opposing the change in magnetization (resulting in a plateau in ΔS_{CC}) which helps to explain the functional form of the directly measured latent heat. In sample G, the product of the two terms results in an initial increase in the ΔS_{CC} estimate when dominated by the changes in phase line slope, followed by a decrease where the decreasing change in magnetization dominates. Although the ΔS_{CC} taken from the magnetization data reproduces the functional form of the directly measured latent heat contribution, as shown in Fig. 7(b), the magnitude estimated from the CC equation is significantly larger. We find that the closest agreement

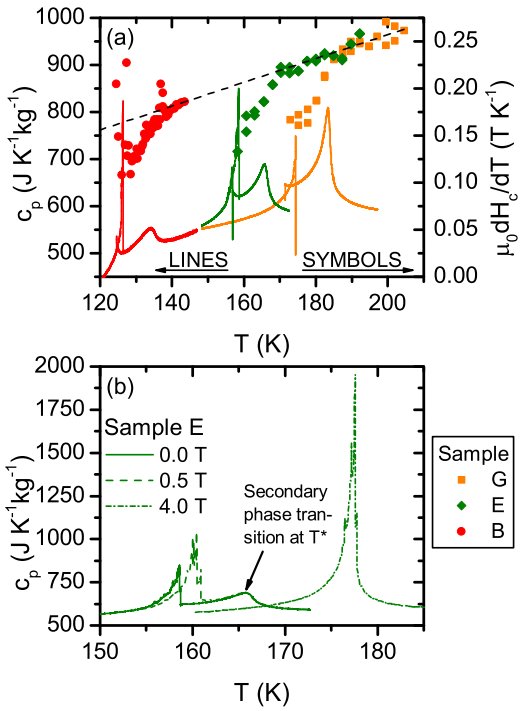

FIG. 8. (a) ac heat capacity of the samples without hydrogen in zero magnetic field shows a peak in heat capacity above the FOPT. The $\mu_0 dH_C/dT$ derived from the measurements on the same fragments is also shown. (b) The peak is not affected by small field; however, it does not exist in the FM state confirming that it is associated with the primary phase. The sharp increase in $\mu_0 dH_C/dT$ is associated with the absorption of this peak as the FOPT is shifted to higher temperatures in field.

can be realized by (a) using fragment samples for both types of measurement and (b) defining the ΔM change by performing minor M-H hysteresis loops, as described in Sec. II B and shown in Fig. 1(b), to establish the precise field and corresponding M at which irreversibility (hysteresis) sets in. These additional measurements are indicated in Fig. 7(b). Previously a fitting routine was used to extract ΔM to perform an estimate of ΔS_{CC} but here too the difficulty in direct extraction, once the transition became only weakly first order, was discussed [38]. If we re-evaluate $\Omega(1.5\ \mathrm{T})$ using the ΔS_{CC} determined for fragment samples we get values of 0.63 and 0.8 for samples E and G, respectively, improving to 0.75 for the latter when the minor hysteresis loop method is used. These issues, particularly the large discrepancy for more weakly first-order transitions, set out the limitation of the Ω parameter.

An interesting observation in these samples is the large changes in phase line slope which are unusual. They appear related to a secondary non-field-driven phase transition above T_C at a temperature T^*, which is present in the heat capacity data shown in Fig. 8. Once the FOPT moves beyond this peak the phase line slope seems to fall on a universal line across the series. The fact that the phase transition at T^* exists at low magnetic fields, but as the field is increased and the FM transition moves to higher temperature, the feature is incorporated into the main ferromagnetic transition, as shown in Fig. 8(b), suggests the peak is of magnetic origin. The change of slope of the $\mu_0 dH_C/dT$ at the temperature where the T_C and T^* coincide supports this statement. Recently [8] it was shown from density functional theory that Mn adds antiferromagnetically into the $La(Fe, Si)_{13}$ lattice, and hence it is tempting to attribute this feature to an AFM ordering of regions of the sample where the Mn resides. We also speculate that the Néel temperature T_N of these regions is influenced by the size of the region, as the transition appears to broaden for samples with more Mn overall. Although this is a low field oddity, only observed due to the sensitivity of our calorimeter, the feature appears to affect the shape of the $\mu_0 dH_C/dT$ and therefore has some influence on the overall magnetocaloric entropy change.

IV. SUMMARY

We have studied a series of Mn doped $La(Fe, Si)_{13}$ samples to examine the explicit change of first-order character in the presence of magnetic field and temperature. We show the dramatic change of the character of the transition when the samples are hydrogenated. Remarkably, although the character of the transition is an important property for the development of the field, no one simple model exists to identify the nature of the transition across different material families and the defining sharp features are usually broadened by material inhomogeneity. Using a direct method we have measured the latent heat of the transition, and introduce a new model independent parameter to define the degree of first-order character explicitly. The use of the parameter will allow different material families to be compared directly, in principle, although it is open to considerable inaccuracy for weakly first-order transitions. In addition, we find an interesting feature in the heat capacity associated with the presence of Mn in the samples.

ACKNOWLEDGMENT

This work is in part funded by the European Community's 7th Framework Programme under Grant Agreement 310748 DRREAM, and the UK EPSRC Grant No. EP/G060940/1

[1] A. Fujita and K. Fukamichi, Giant volume magnetostriction due to the itinerant electron metamagnetic transition in La(Fe-Si)$_{13}$ compounds, IEEE Trans. Magn. **35**, 3796 (1999).

[2] A. Fujita, S. Fujieda, Y. Hasegawa, and K. Fukamichi, Itinerant-electron metamagnetic transition and large magnetocaloric effects in $La(Fe_xSi_{1-x})_{13}$ compounds and their hydrides, Phys. Rev. B **67**, 104416 (2003).

[3] M. Kuepferling, V. Basso, C. P. Sasso, L. Giudici, J. D. Moore, K. Morrison, and L. F. Cohen, Hall imaging of the history dependence of the magnetocaloric effect in $Gd_5Si_{2.09}Ge_{1.91}$, IEEE Trans. Magn. **44**, 3233 (2008).

[4] T. Krenke, S. Aksoy, E. Duman, M. Acet, X. Moya, L. Mañosa, and A. Planes, Hysteresis effects in the magnetic-field-induced

reverse martensitic transition in magnetic shape-memory alloys, J. Appl. Phys. **108**, 043914 (2010).

[5] V. Basso, C. P. Sasso, K. P. Skokov, O. Gutfleisch, and V. V. Khovaylo, Hysteresis and magnetocaloric effect at the magnetostructural phase transition of Ni-Mn-Ga and Ni-Mn-Co-Sn Heusler alloys, Phys. Rev. B **85**, 014430 (2012).

[6] S. Fujieda, A. Fujita, K. Fukamichi, Y. Yamazaki, and Y. Iijima, Giant isotropic magnetostriction of itinerant-electron metamagnetic $La(Fe_{0.88}Si_{0.12})_{13}H_y$ compounds, Appl. Phys. Lett. **79**, 653 (2001).

[7] S. Fujieda, A. Fujita, and K. Fukamichi, Strong pressure effect on the Curie temperature of itinerant-electron metamagnetic $La(Fe_{0.88}Si_{0.12})_{13}H_y$ and $La_{0.7}Ce_{0.3}(Fe_{0.88}Si_{0.12})_{13}H_y$, Mater. Trans. **50**, 483 (2009).

[8] Z. Gercsi, Magnetic coupling in transition-metal-doped $LaSiFe_{11.5}TM_{0.5}$ (TM = Cr, Mn and Ni), Europhys. Lett. **110**, 47006 (2015).

[9] F. Wang, Y. F. Chen, G. J. Wang, J. R. Sun, and B. G. Shen, Large magnetic entropy change and magnetic properties in $La(Fe_{1-x}Mn_x)_{11.7}Si_{1.3}H_y$ compounds, Chinese Phys. **12**, 911 (2003).

[10] A. Barcza, M. Katter, V. Zellmann, S. Russek, S. Jacobs, and C. Zimm, Stability and magnetocaloric properties of sintered $La(Fe,Mn,Si)_{13}H_z$ alloys, IEEE Trans. Magn. **47**, 3391 (2011).

[11] M. Krautz, K. Skokov, T. Gottschall, C. S. Teixeira, A. Waske, J. Liu, L. Schultz, and O. Gutfleisch, Systematic investigation of Mn substituted $La(Fe,Si)_{13}$ alloys and their hydrides for room-temperature magnetocaloric application, J. Alloys Compd. **598**, 27 (2014).

[12] F. Wang, Y. F. Chen, G. J. Wang, and B. G. Shen, The effect of Mn substitution in $LaFe_{11.7}Si_{1.3}$ compound on the magnetic properties and magnetic entropy changes, J. Phys. D **36**, 1 (2003).

[13] S. I. Makarov, M. Krautz, S. Salamon, K. Skokov, C. S. Teixeira, O. Gutfleisch, H. Wende, and W. Keune, Local electronic and magnetic properties of pure and Mn-containing magnetocaloric $LaFe_{13-x}Si_x$ compounds inferred from Mössbauer spectroscopy and magnetometry, J. Phys. D: Appl. Phys. **48**, 305006 (2015).

[14] B. K. Banerjee, On a generalised approach to first and second order magnetic transitions, Phys. Lett. **12**, 16 (1964).

[15] A. Arrott, Criterion for ferromagnetism from observations of magnetic isotherms, Phys. Rev. **108**, 1394 (1957).

[16] C. P. Bean and D. S. Rodbell, Magnetic disorder as a first-order phase transformation, Phys. Rev. **126**, 104 (1962).

[17] V. Basso, The magnetocaloric effect at the first-order magnetoelastic phase transition, J. Phys.: Condens. Matter **23**, 226004 (2011).

[18] M. Shimizu, Rep. Prog. Phys. **44**, 329 (1981).

[19] T. Moriya, On the possible mechanisms for temperature-induced ferromagnetism, J. Phys. Soc. Jpn. **55**, 357 (1986).

[20] V. S. Amaral and J. S. Amaral, Magnetoelastic coupling influence on the magnetocaloric effect in ferromagnetic materials, J. Magn. Magn. Mater. **272–276**, 2104 (2004).

[21] J. D. Moore, K. Morrison, K. G. Sandeman, M. Katter, and L. F. Cohen, Reducing extrinsic hysteresis in first-order $La(Fe,Co,Si)_{13}$ magnetocaloric systems, Appl. Phys. Lett. **95**, 252504 (2009).

[22] E. Lovell, A. M. Pereira, A. D. Caplin, J. Lyubina, and L. F. Cohen, Dynamics of the first-order metamagnetic transition in magnetocaloric $La(Fe,Si)_{13}$: Reducing hysteresis, Adv. Energy Mater. **5**, 1401639 (2015).

[23] K. Morrison and L. F. Cohen, Overview of the characteristic features of the magnetic phase transition with regards to the magnetocaloric effect: The hidden relationship between hysteresis and latent heat, Metal. Mater. Trans. E **1**, 153 (2014).

[24] V. Basso, M. Kuepferling, C. Curcio, C. Bennati, A. Barzca, M. Katter, M. Bratko, E. Lovell, J. Turcaud, and L. F. Cohen, Specific heat and entropy change at the first-order phase transition of $La(Fe\text{-}Mn\text{-}Si)_{13}$-H compounds, J. Appl. Phys. **118**, 053907 (2015).

[25] A. M. Tishin and Y. I. Spichkin, *The Magnetocaloric Effect and Its Applications* (Institute of Physics, Bristol, 2003).

[26] M. Katter, V. Zellmann, G. Reppel, and K. Uestuener, Magnetocaloric properties of $La(Fe,Co,Si)_{13}$ bulk material prepared by powder metallurgy, IEEE Trans. Magn. **44**, 3044 (2008).

[27] E Lovell, L Ghivelder, A. Nicotina, J. Turcaud, M. Bratko, A. D. Caplin, V. Basso, A. Barcza, M. Katter, and L. F. Cohen, Low-temperature specific heat in hydrogenated and Mn-doped $La(Fe,Si)_{13}$, Phys. Rev. B **94**, 134405 (2016).

[28] L. Caron, Z. Q. Ou, T. T. Nguyen, D. T. C. Thanh, O. Tegus, and E. Bruck, On the determination of the magnetic entropy change in materials with first-order transitions, J. Magn. Magn. Mater. **321**, 3559 (2009).

[29] M. Bratko, K. Morrison, A. de Campos, S. Gama, L. F. Cohen, and K. G. Sandeman, History dependence of directly observed magnetocaloric effects in (Mn, Fe)As, Appl. Phys. Lett. **100**, 252409 (2012).

[30] A. A. Minakov, S. B. Roy, Y. V. Bugoslavsky, and L. F. Cohen, Thin-film alternating current nanocalorimeter for low temperatures and high magnetic fields, Rev. Sci. Instrum. **76**, 043906 (2005).

[31] Y. Miyoshi, K. Morrison, J. D. Moore, A. D. Caplin, and L. F. Cohen, Heat capacity and latent heat measurements of CoMnSi using a microcalorimeter, Rev. Sci. Instrum. **79**, 074901 (2008).

[32] K. Morrison, M. Bratko, J. Turcaud, A. Berenov, A. D. Caplin, and L. F. Cohen, A calorimetric method to detect a weak or distributed latent heat contribution at first order magnetic transitions, Rev. Sci. Instrum. **83**, 033901 (2012).

[33] K. Morrison, J. Lyubina, J. D. Moore, A. D. Caplin, K. G. Sandeman, O. Gutfleisch, and L. F. Cohen, Contributions to the entropy change in melt-spun $LaFe_{11.6}Si_{1.4}$, J. Phys. D **43**, 132001 (2010).

[34] K. Morrison, J. Lyubina, J. D. Moore, K. G. Sandeman, O. Gutfleisch, L. F. Cohen, and A. D. Caplin, Magnetic refrigeration: Phase transitions, itinerant magnetism and spin fluctuations, Philos. Mag. **92**, 292 (2012).

[35] V. I. Zverev, A. M. Tishin, and M. D. Kuz'min, The maximum possible magnetocaloric ΔT effect, J. Appl. Phys. **107**, 043907 (2010).

[36] K. G. Sandeman, Magnetocaloric materials: The search for new systems, Scr. Mater. **67**, 566 (2012).

[37] J. Liu, T. Gottschall, K. P. Skokov, J. D. Moore, and O. Gutfleisch, Giant magnetocaloric effect driven by structural transitions, Nat. Mater. **11**, 620 (2012).

[38] A. Fujita and K. Fukamichi, Enhancement of isothermal entropy change due to spin fluctuations in itinerant-electron metamagnetic $La(Fe_{0.88}Si_{0.12})_{13}$ compound, J. Alloys Compd. **408–412**, 62 (2006).